

Rhenium mixed-ligand complexes with *S,N,S*-tridentate thiosemicarbazone/thiosemicarbazide ligand†Cite this: *Dalton Trans.*, 2013, **42**, 5111Pedro I. da S. Maia,^a Hung Huy Nguyen,^b Adelheid Hagenbach,^c Silke Bergemann,^d Ronald Gust,^e Victor M. Deflon^a and Ulrich Abram^{*c}

Rhenium(v) complexes containing tridentate thiosemicarbazones/thiosemicarbazides (H₂L1) derived from *N,N',N'*-dialkylamino(thiocarbonyl)benzimidoyl chlorides with 4,4-dialkylthiosemicarbazides have been synthesized by ligand-exchange reactions starting from [ReOCl(L1)]. The chlorido ligand of [ReOCl(L1)] (**4**) is readily replaced and reactions with ammonium thiocyanate or potassium cyanide give [ReO(NCS)(L1)] (**6**) and [ReO(CN)(L1)] (**7**), respectively. The reaction of (NBu₄)[ReOCl₄] with H₂L1 and two equivalents of ammonium thiocyanate, however, gives in a one-pot reaction [ReO(NCS)₂(HL1)] (**8**), in which the pro-ligand H₂L1 is only singly deprotonated. An oxo-bridged, dimeric nitridorhenium(v) compound of the composition [(ReN(HL1))₂O] (**11**) is obtained from a reaction of (NBu₄)[ReOCl₄], H₂L1 and sodium azide. The six-coordinate complexes [ReO(L1)(Ph₂btu)] (**12**), where HPh₂btu is *N,N*-diphenyl-*N'*-benzoylthiourea, can be obtained by treatment of [ReOCl(L1)] with HPh₂btu in the presence of NEt₃. Studies of the antiproliferative effects of the [ReOX(L1)] system (X = Cl⁻, NCS⁻ or CN⁻) on breast cancer cells show that the lability of a monodentate ligand seems to play a key role in the cytotoxic activity of the metal complexes, while the substitution of this ligand by the chelating ligand Ph₂btu⁻ completely terminates the cytotoxicity.

Received 8th December 2012,

Accepted 29th January 2013

DOI: 10.1039/c3dt32950j

www.rsc.org/dalton

Introduction

Thiosemicarbazones and their transition metal complexes are versatile compounds and some of them possess remarkable biological and pharmaceutical properties including anti-neoplastic activity.^{1–6} Relatively less is known about thiosemicarbazones with rhenium and technetium. This is surprising since some of the hitherto explored compounds have shown that they are able to stabilize the {M^V=O}³⁺ and M³⁺ (M = Re, Tc) cores, which are readily accessible by reduction of [MO₄]⁻ ions from commercial isotope generator systems with common reducing agents. This makes them interesting as ligands in future radiopharmaceutical agents, since the two

β⁻-emitting isotopes, ¹⁸⁸Re and ¹⁸⁶Re, have potential to be used in radioimmunotherapy,^{7–9} while the radionuclide ^{99m}Tc is widely used in diagnostic nuclear medicine.^{10–13} Additionally, some of the hitherto isolated thiosemicarbazone complexes of rhenium possess intrinsic anticancer properties, but the molecular mechanism of interaction is not yet known.^{14,15}

Surprisingly, the first structural report on rhenium thiosemicarbazone complexes was published only in 2003 dealing with cationic Re^{III} compounds of the general composition [Re^{III}(L)₂]⁺ (**1**, Chart 1), with HL = 2-acetylpyridine thiosemicarbazones. They were prepared by a reductive ligand exchange

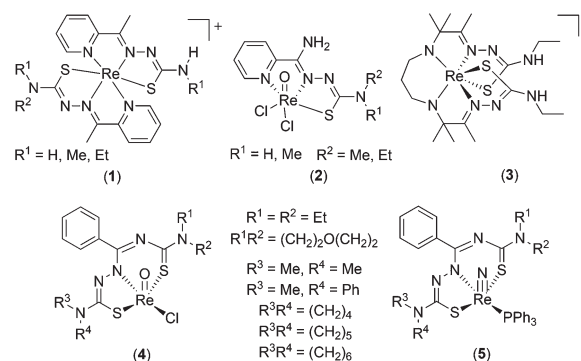


Chart 1 Rhenium complexes with thiosemicarbazones (for details see ref. 14–19).

^aInstituto de Química de São Carlos, Universidade de São Paulo, CP 780, São Carlos-SP, Brazil

^bDepartment of Chemistry, Hanoi University of Sciences, 19 Le Thanh Tong, Hanoi, Vietnam

^cInstitute of Chemistry and Biochemistry, Freie Universität Berlin, Fabeckstraße 34/36, 14195 Berlin, Germany. E-mail: Ulrich.abram@fu-berlin.de;

Fax: +49 30 83852676; Tel: +49 30 83854002

^dInstitute of Pharmacy, Freie Universität Berlin, Königin-Luise-Str. 2+4, 14195 Berlin, Germany

^eInstitute of Pharmacy, University Innsbruck, Innrain 80/82, A-6020 Innsbruck, Austria

†CCDC 911727–911733. For crystallographic data in CIF or other electronic format see DOI: 10.1039/c3dt32950j

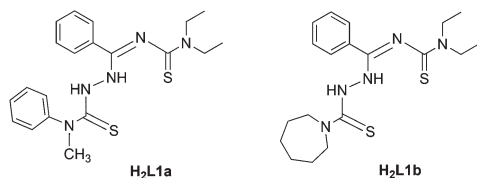


Chart 2 Thiosemicarbazone ligands used in this study.

starting from $[\text{ReOCl}_3(\text{PPh}_3)_2]$ or perrhenate.¹⁶ However, a number of undesired side-reactions complicated the isolation of higher amounts of pure products in such procedures. The stabilization of oxorhenium(v) complexes of the composition $[\text{ReOCl}_2(\text{L})]$ (**2**) succeeded with HL = 2-acetylpyridineformamide thiosemicarbazones.¹⁷ Reduction of the metal ion and the formation of Re^{III} complexes, here, occur only when an excess of thiosemicarbazones is used and the reaction is performed for a prolonged period of time.¹⁷ Very recently, a cationic rhenium(v) complex of the composition $[\text{Re}(\text{L})]^+$ (**3**) with a hexadentate bis(thiosemicarbazone) ligand (H_4L) was prepared.¹⁸ Compound **3** represents a rare example of a rhenium(v) complex, which does not contain one of the ReO^{3+} , ReN^{2+} or $\text{Re}(\text{NPh})^{3+}$ cores, but coordinates the hexadentate ligand with a distorted trigonal prismatic coordination sphere.

In previous papers we reported some representatives of a new class of rhenium(v) and technetium(v) complexes with tridentate thiosemicarbazones/thiosemicarbazides ($\text{H}_2\text{L1}$), which contain an additional thiourea binding site.¹⁴ They stabilize the MO^{3+} ($\text{M} = \text{Re}$ and Tc) as well as ReN^{2+} cores upon formation of complexes of the compositions $[\text{MOCl}(\text{L1})]$ ($\text{M} = \text{Re}$; **4**) and $[\text{ReN}(\text{L1})(\text{PPh}_3)]$ (**5**), respectively. A significant cell growth inhibition of human MCF-7 breast cancer cells was observed in *in vitro* experiments for several representatives of $\text{H}_2\text{L1}$ and their oxorhenium(v) complexes $[\text{ReOCl}(\text{L1})]$.¹⁵ No clear structure–activity relationship (SAR) of compounds **4** was observed when the periphery of the thiosemicarbazones was modified (neither in the positions R^1 and R^2 nor in the positions R^3 and R^4), while the replacement of the O^{2-} ligand by a nitrido N^{3-} ligand and the chlorido ligand by a triphenylphosphine (compound **5** in Chart 1) terminates the cytotoxicity of the complexes.

In the present communication, we describe the ligand exchange chemistry of $[\text{ReOCl}(\text{L1})]$ complexes together with some evaluation of the biological activity of the reaction products. Two ligands with methyl/phenyl ($\text{H}_2\text{L1a}$) and hexamethylene ($\text{H}_2\text{L1b}$) residues (see Chart 2) in the thiosemicarbazone binding site have been used throughout the experiments, while the thiourea binding site was kept unchanged with two ethyl residues.

Results and discussions

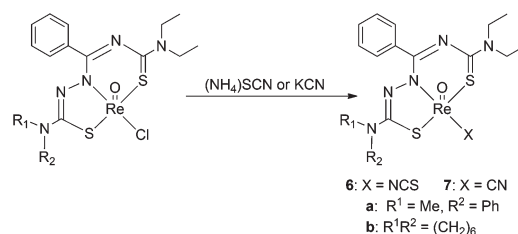
The chlorido ligand in the $[\text{ReOCl}(\text{L1})]$ complexes is sufficiently labile to allow ligand exchange reactions under mild conditions. Reactions of $[\text{ReOCl}(\text{L1})]$ with ammonium

thiocyanate or potassium cyanide in $\text{MeOH}-\text{CH}_2\text{Cl}_2$ give red complexes of the types $[\text{ReO}(\text{NCS})(\text{L1})]$ (**6**) and $[\text{ReO}(\text{CN})(\text{L1})]$ (**7**) (Scheme 1), respectively, in high yields. Attempts to prepare the analogous isoselenocyanato compound failed, since the corresponding reaction with KSeCN resulted in the precipitation of elemental selenium and only the cyanido complexes $[\text{ReO}(\text{CN})(\text{L1})]$ could be isolated in medium yields. The products are readily soluble in CH_2Cl_2 and only sparingly soluble in MeOH .

The IR spectra of isothiocyanato derivatives **6** show strong bands around 2060 cm^{-1} , which is in accord with the coordination through the nitrogen atoms of isothiocyanato ligands.¹⁹ N-coordination of the NCS^- is found for the majority of rhenium complexes with this ligand.²⁰ The $\nu_{(\text{CN})}$ stretches in the IR spectra of the complexes **7** are detected as weak bands in the $2120\text{--}2130\text{ cm}^{-1}$ region. These observations are in agreement with the fact that the CN^- ion is a better σ -donor than a π -acceptor. Thus, a shift to higher wavenumbers of the $\nu_{(\text{CN})}$ frequency with regard to uncoordinated cyanide (2080 cm^{-1}) is observed when electrons are removed from the 5σ orbital, which is weakly antibonding.¹⁹ Furthermore, the strong $\text{Re}=\text{O}$ vibrations are observed around 975 and 990 cm^{-1} for the $[\text{ReO}(\text{NCS})(\text{L1})]$ and $[\text{ReO}(\text{CN})(\text{L1})]$ complexes, respectively.

The ^1H NMR spectra of **6** and **7** are expectedly very similar to those of $[\text{ReOCl}(\text{L1})]$. The ESI^+ MS spectra of all compounds show the molecular ion peaks. While these peaks are the exclusive high-mass peaks in the spectra of the cyanido compounds, the spectra of the $[\text{ReO}(\text{NCS})(\text{L1})]$ show additional intense peaks for ions, which can be attributed to $[\text{ReO}(\text{L1})]^+$. This indicates relatively weak $\text{Re}-\text{N}$ bonds.

X-ray structure analyses confirm the spectroscopic data. Fig. 1a illustrates the molecular structure of **6a** as a representative of the $[\text{ReO}(\text{NCS})(\text{L1})]$ complexes. Selected bond lengths and angles for this compound are shown together with the values for **6b** (not shown) in Table 1. The asymmetric unit of **6a** contains two molecules, which are different in the orientation of their two ethyl residues. In one of the molecules the ethyl groups are positioned in the same direction as the $\text{Re}=\text{O}$ bond, while in the second one they point to the opposite direction. Fig. 1b illustrates the molecular structure of $[\text{ReO}(\text{CN})(\text{L1a})]$ (**7a**) as a representative compound of the cyanido derivatives. For all three studied complexes, the coordination environments of the rhenium atoms are best described as distorted square pyramids, where the oxo ligands occupy the apical positions and the basal planes are defined by the donor atoms of the tridentate thiosemicarbazone



Scheme 1 Reactions of $[\text{ReOCl}(\text{L1})]$ with pseudohalides.

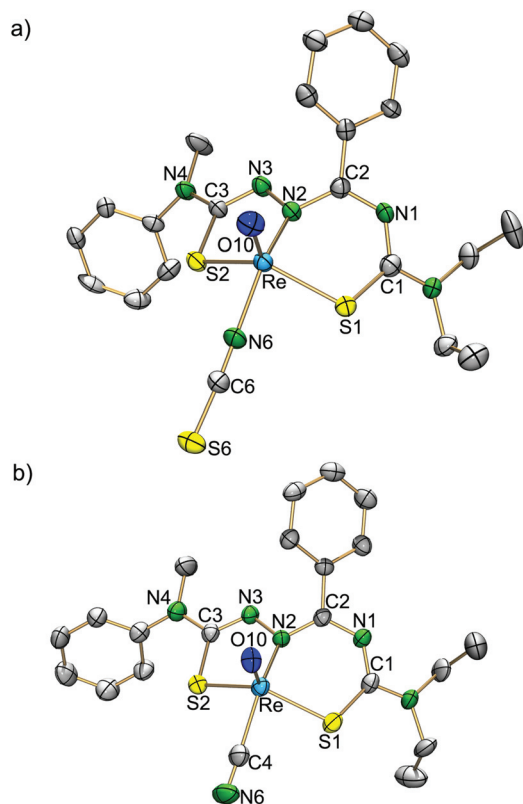


Fig. 1 Ellipsoid representations of the molecular structures of (a) [ReO(NCS)(L1a)] (**6a**) and (b) [ReO(CN)(L1a)] (**7a**).²¹ Hydrogen atoms have been omitted for clarity.

Table 1 Selected bond lengths (Å) and angles (°) for [ReO(NCS)(L1a)]^a (**6a**), [ReO(NCS)(L1b)] (**6b**) and [ReO(CN)(L1a)] (**7a**)

	6a	6b	7a
Re–O10	1.664(6)/1.670(6)	1.65(2)	1.686(5)
Re–S1	2.310(2)/2.313(2)	2.293(8)	2.295(2)
Re–S2	2.275(2)/2.271(2)	2.278(4)	2.285(2)
Re–N2	1.982(5)/1.999(6)	2.05(1)	2.023(5)
Re–N6	2.045(6)/2.040(7)	2.07(2)	
Re–C4			2.051(8)
S1–C1	1.753(8)/1.738(8)	1.79(2)	1.751(7)
C1–N1	1.343(9)/1.345(9)	1.29(3)	1.337(8)
N1–C2	1.308(9)/1.325(9)	1.33(2)	1.314(7)
C2–N2	1.380(9)/1.368(9)	1.33(2)	1.352(8)
N2–N3	1.415(8)/1.416(8)	1.40(2)	1.411(7)
N3–C3	1.29(1)/1.28(1)	1.30(2)	1.298(8)
S2–C3	1.777(7)/1.785(7)	1.79(2)	1.765(7)
C3–N4	1.36(1)/1.36(1)	1.30(2)	1.367(8)
O10–Re–S1	112.4(2)/112.6(2)	109.5(5)	112.2(2)
O10–Re–N2	104.6(3)/104.0(3)	108.4(7)	107.9(2)
O10–Re–S2	113.7(2)/113.3(2)	110.4(5)	113.4(2)
O10–Re–N6	104.6(3)/104.4(3)	104.8(9)	
O10–Re–C4			103.6(3)

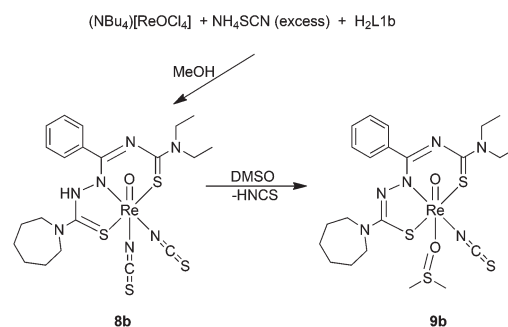
^a Values for two crystallographically independent molecules.

ligands and the donor atom of the pseudohalide. Five-coordination is not rare in the coordination chemistry of oxorhenium(v) or nitridorhenium(v) complexes,²⁰ and is due to the strong and space-filling π -donors O^{2-} and N^{3-} . Their coordination

results in increased O/N-M-(equatorial) donor atom angles. This is also observed in the examples of the present communication, where values between 103.6(3) and 113.7(2)° are observed (Table 1). Consequently, the rhenium atoms are situated above the least square planes of the equatorial donors (0.769(3) and 0.767(3) Å for **6a**, 0.679(6) Å for **6b** and 0.721(2) Å for **7a**). In the isothiocyanato complexes, the CS bonds in the isothiocyanato ligands are shorter than those in the thiosemicarbazonato ion, which is indicative of a delocalization of π -electron density inside the almost linear NCS^- ligand. Both the Re–CN and Re–NCS bond lengths are around 2.05 Å.

In the complexes discussed above, in the rhenium(v) complexes of ref. 15 as well as in the corresponding Au(III) complexes of the composition [AuCl(L1)],²² the tridentate ligands are always doubly deprotonated, which provides an optimal charge compensation. During reactions with M^{2+} ions, such as Ni^{2+} , Pd^{2+} or Pt^{2+} , however, H_2L1 ligands form square-planar complexes of the same topology ([MCl(HL1)]), but with one deprotonation only. Thus, they are obviously able to act in accordance with the charge requirements of the metal complexes formed. This has also been observed for isothiocyanato complexes with the oxorhenium(v) core. While the five-coordinate compounds [ReO(NCS)(L1)] described above are results of Cl^-/NCS^- ligand exchange reactions and do not undergo further reactions even with an excess of SCN^- , another reaction pathway is observed when the reaction conditions are modified.²³ One-pot reactions of $(NBu_4)[ReOCl_4]$ with H_2L1b and an excess of NH_4SCN reproducibly result in a brown complex of the composition [ReO(NCS)₂(HL1b)] (**8b**), in which only a single deprotonation of the chelator is observed. The reaction is almost quantitative. The resulting neutral complex is readily soluble in CH_2Cl_2 or $CHCl_3$, but almost insoluble in alcohols (Scheme 2).

The IR spectrum of **8b** expectedly shows signals of two NCS^- ligands with considerably different bonding positions, which is finally confirmed by the results of an X-ray structure analysis. The Re=O stretching vibration is observed at 965 cm^{-1} , which is hypsochromically shifted by 15 cm^{-1} with respect to the value in the IR spectrum of **6b**. This can be explained by the occupation of the coordination position *trans* to the oxido ligand by another NCS^- . The weaker bond to the axial NCS^- ligand is also confirmed by X-ray diffraction (Re–N6



Scheme 2 Formation of [ReO(NCS)₂(HL1b)] (**8b**) and [ReO(NCS)(DMSO)(L1b)] (**9b**).

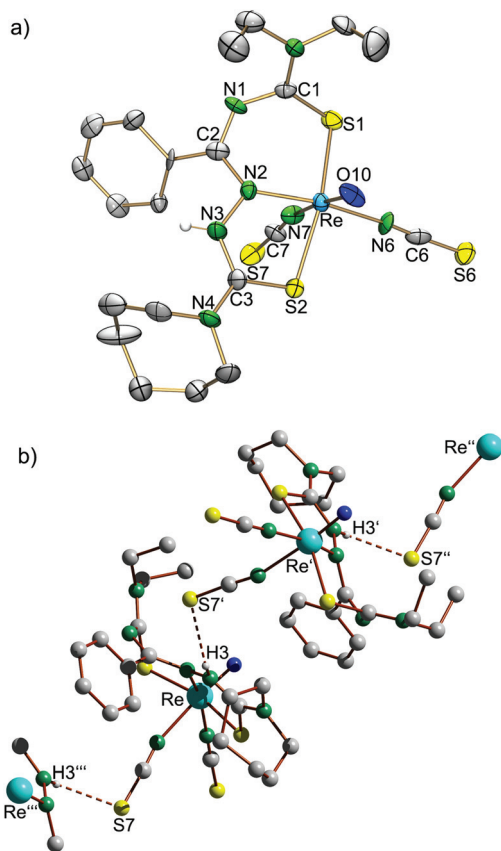


Fig. 2 (a) Ellipsoid representations of the molecular structure of $[\text{ReO}(\text{NCS})_2(\text{HL1b})]$ (**8b**).²¹ Hydrogen atoms on carbon atoms have been omitted for clarity. (b) Hydrogen bonding: $\text{N3}\cdots\text{S7}'$ 3.261 Å, $\text{N3-H3}\cdots\text{S7}'$ 144.6°, symmetry operation ('): $x + 3/2, y - 1/2, -z + 1/2$.²⁴

bond: 2.10(1) Å vs. Re-N7 : 2.21(1) Å). Fig. 2a depicts the molecular structure of **8b**. Table 2 summarizes selected bond lengths and angles. It can clearly be seen that the bonding situation in the complex is changed by the increase of the coordination number. The O10-Re-N/S angles to the donor atoms of the equatorial coordination sphere decrease and, thus, the rhenium atom is shifted out of the equatorial coordination plane by 0.283(5) Å towards the oxido ligand. But also the bond lengths inside the chelating ligand are changed as a consequence of the protonation of N3. The C3–N3 bond, but also the C–S bonds are lengthened with respect to **6b**.

The lability of the NCS^- ligand in *trans* position to the oxido ligand in $[\text{ReO}(\text{NCS})_2(\text{HL1b})]$ (**8b**) is demonstrated by the formation of $[\text{ReO}(\text{NCS})(\text{dmsO-}\kappa\text{O})(\text{L1b})]$ (**9b**), when the bis-isothiocyanato compound is recrystallized from DMSO. The replacement of the anionic ligand NCS^- by a neutral dmsO ligand in *trans* position to the oxido ligand goes along with a second deprotonation of the organic ligand in **8b**. This type of reaction underlines the flexibility of the tridentate H_2L ligands to act as mono- or dianionic chelators in dependence on the requirements of the coordinated metal ions. Such behaviour has also been observed with other metal ions before as discussed above. The solid state structure of **8b** contains hydrogen bonds

Table 2 Selected bond lengths (Å) and angles (°) for $[\text{ReO}(\text{NCS})_2(\text{HL1b})]$ (**8b**) and $[\text{ReO}(\text{NCS})(\text{dmsO-}\kappa\text{O})(\text{L1b})]$ (**9b**)^a

	8b	9b
Re–O10	1.68(1)	1.674(6)/1.658(6)
Re–S1	2.370(4)	2.368(2)/2.55(2)
Re–S2	2.377(3)	2.332(2)/2.340(2)
Re–N2	2.00(1)	2.012(6)/2.009(6)
Re–N6	2.10(1)	2.048(7)/2.066(7)
Re–N7	2.21(1)	—
Re–O20	—	2.265(6)/2.274(5)
S1–C1	1.73(1)	1.753(8)/1.755(8)
C1–N1	1.39(2)	1.32(1)/1.322(9)
N1–C2	1.301(2)	1.33(1)/1.340(9)
C2–N2	1.43(2)	1.34(1)/1.339(9)
N2–N3	1.42(2)	1.428(9)/1.446(8)
N3–C3	1.36(2)	1.30(1)/1.29(1)
S2–C3	1.71(2)	1.763(8)/1.787(8)
C3–N4	1.34(2)	1.37(1)/1.355(9)
O10–Re–S1	96.9(3)	98.6(2)/100.2(2)
O10–Re–N2	100.8(6)	100.6(3)/100.5(3)
O10–Re–S2	99.1(3)	100.6(2)/100.2(2)
O10–Re–N6	92.7(6)	97.5(3)/97.0(3)
O10–Re–N7	172.7(6)	—
O10–Re–O20	—	177.2(3)/176.3(2)

^a Values for two crystallographically independent species.

between N3 and the sulfur atom of the NCS^- ligand in *trans* position of the oxido ligand (see Fig. 2b), and thus, pre-formed HSCN. Despite the fact that this is an intermolecular hydrogen bond and only present in the solid state, it cannot be excluded that the related weakening of the Re-N7 bond supports the abstraction of HSCN during the dissolution of **8b** in DMSO.

The molecular structure of **9b** is shown in Fig. 3. Selected bond lengths and angles are compared to the corresponding values of **8b** in Table 2. The second deprotonation of the organic ligands causes the re-formation of an extended π -system with C–N and C–S bond lengths being between the values expected for the respective single or double bonds. The dmsO ligand is O-bonded as in almost all of the few structurally characterized dmsO complexes of rhenium.^{25–30} The only exception, where an S-bonded dmsO ligand has unambiguously been found in a rhenium compound, is the organo-metallic complex $[\text{Re}(\text{NO})(\text{cp})(\text{PPh}_3)(\text{dmsO-}\kappa\text{S})]^+$.³¹

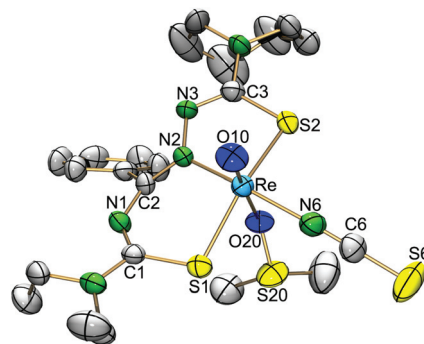
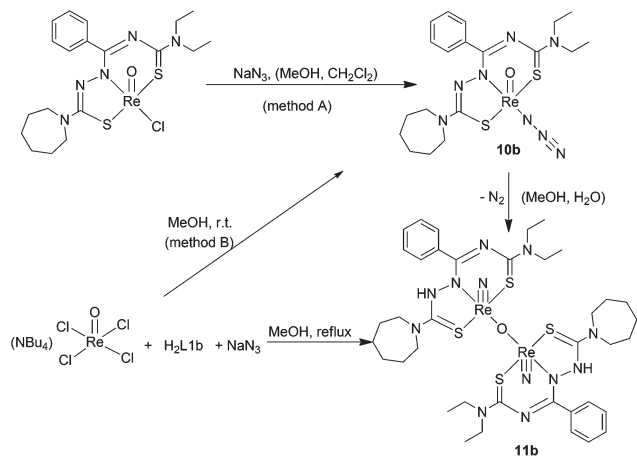


Fig. 3 Ellipsoid representations of the molecular structure of $[\text{ReO}(\text{NCS})(\text{dmsO-}\kappa\text{O})(\text{L1b})]$ (**9b**).²¹ Hydrogen atoms have been omitted for clarity.



Scheme 3 Formation of $[\{\text{ReN}(\text{HL}1\text{b})\}_2\text{O}]$ (**11b**).

The exchange of the chlorido ligand in $[\text{ReOCl}(\text{L}1\text{b})]$ can also be performed by an azido one. The resulting product $[\text{ReO}(\text{N}_3)(\text{L}1\text{b})]$ (**10b**) can be isolated from two reactions: (i) the ligand exchange starting from $[\text{ReOCl}(\text{L}1\text{b})]$ with sodium azide in a CH_2Cl_2 -MeOH mixture or (ii) by a one-pot reaction starting from $(\text{NBU}_4)[\text{ReOCl}_4]$, NaN_3 and $\text{H}_2\text{L}1\text{b}$ in MeOH (Scheme 3). The product precipitates as a brown solid in both cases. The IR spectrum of **10b** shows the $\nu_{(\text{Re}=\text{O})}$ vibration at 972 cm^{-1} and a strong band related to $\nu_{(\text{N}=\text{N})}$ at 2059 cm^{-1} , which is in the expected range for an azido ligand in the equatorial plane of a rhenium(v) complex.³² In solution, however, **10b** is not stable and the formation of a nitrido species is observed. For this reason, method B is recommended for the synthesis of **10b**. The formation of HCl during the synthesis according to method A may facilitate the conversion into the nitrido complex. The conversion of the azido compound into a nitrido complex proceeds even at room temperature and also prevents the recording of NMR spectra of sufficient quality. After recrystallization from CH_2Cl_2 -MeOH or CH_2Cl_2 -MeCN, deep red crystals of the composition $[\{\text{ReN}(\text{HL}1\text{b})\}_2\text{O}]$ (**11b**) are obtained. In the IR spectrum of these crystals no more $\nu_{(\text{Re}=\text{O})}$ and $\nu_{(\text{N}=\text{N})}$ vibrations are present, but a new band at 694 cm^{-1} indicates the possible formation of a μ -oxo dimeric complex. A band at 1028 cm^{-1} can be assigned to the $\nu_{(\text{Re}=\text{N})}$ vibration.^{33,34}

The decomposition of nitrido ligands or other nitrogen-containing ligands with final formation of nitrido complexes has been described for many examples,^{35–37} and particularly the decomposition of azido compounds is a convenient approach, e.g. to prepare the common nitrido precursor $(\text{NBU}_4)[\text{ReNCl}_4]$.³⁸

The nature of **11b** as an oxo-bridged dimer is confirmed by the high resolution mass spectrometry and X-ray diffraction. The ESI+ MS spectrum of the complex clearly presents the molecular ion peak of the nitrido complex at $m/z = 1198.2446$ (m/z (calcd) = 1198.2698) instead of the oxo ligand (m/z (calcd) = 1200.2378). Fig. 4 shows the molecular structure of the complex, which possesses inversion symmetry with the oxygen

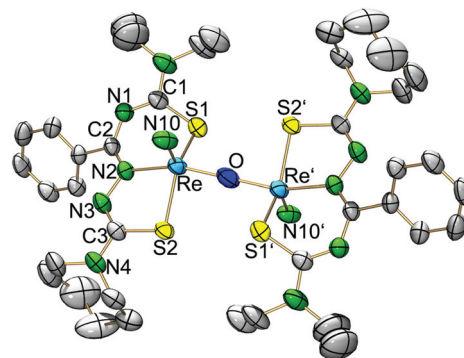


Fig. 4 Ellipsoid representations of the molecular structure of $[\{\text{ReN}(\text{HL}1\text{b})\}_2\text{O}]$ (**11b**).²¹ Hydrogen atoms have been omitted for clarity.

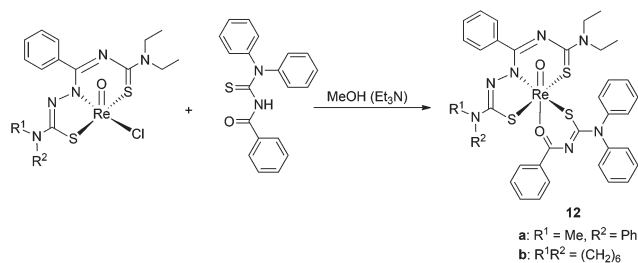
Table 3 Selected bond lengths (Å) and angles (°) for **11b**

Re–N10	1.676(5)	C1–N1	1.316(7)
Re–S1	2.333(2)	N1–C2	1.332(6)
Re–S2	2.315(1)	C2–N2	1.325(6)
Re–N2	2.119(1)	N2–N3	1.418(6)
Re–O	1.829(1)	N3–C3	1.272(7)
S1–C1	1.737(6)	C3–S2	1.769(5)
N10–Re–S1	110.6(2)	S1–Re–N2	87.7(1)
N10–Re–N2	102.7(2)	S1–Re–O	83.98(4)
N10–Re–S2	110.7(2)	S2–Re–N2	80.0(1)
N10–Re–O	106.7(2)	S2–Re–O	87.71(3)
S1–Re–S2	138.55(5)	N2–Re–O	150.5(1)

atom as a centre of inversion. Selected bond lengths and angles are contained in Table 3. The rhenium atoms are five-coordinate, which is a frequent finding in the chemistry of nitridorhenium(v) complexes and readily explained by the strong *trans* influence of the terminal nitrido ligand. The coordination mode of the chelating ligand is unexceptional and similar to that in **8b**. The bridging oxido ligand originates from residual water in the solvent used. Similar reaction patterns have been observed before for other oxorhenium(v) complexes.²⁰

The formation of oxo bridges in *cis* arrangement to a nitrido ligand is not without precedence in the coordination chemistry of rhenium, but is hitherto restricted to one example of a Re(v) complex and some Re(vii) compounds.^{39,40} A few more examples are known for the lighter homologous element technetium, which possesses a more extended nitrido chemistry, and where the $\{\text{NTcO}_2\text{TcN}\}^{2+}$ unit represents a core structure of the Tc(vi) chemistry.^{41–44}

The formation of “3 + 2” mixed ligand complexes could be achieved by reacting $[\text{ReOCl}(\text{L}1)]$ complexes with *N,N*-diphenylbenzoylthiourea, HPh_2btu , in a mixture of CH_2Cl_2 and MeOH (Scheme 4). The bidentate benzoylthiourea has been chosen for such experiments as a representative for other bidentate, monoanionic ligands. We have recently studied the coordination chemistry of these O,S ligands with several rhenium and technetium precursors extensively and could show that



Scheme 4 Formation of the "3 + 2" mixed-ligand complexes.

they form stable complexes with different oxorhenium(v) cores including "3 + 2" mixed-ligand compounds.^{45–49} The reactions, which can simply be performed in a one-pot version without the isolation of the [ReOCl(L1)] complexes, result in purple solids of the general composition [ReO(L1)(Ph₂btu)] (**12**).

The IR spectra of the complexes **12** exhibit $\nu_{(\text{Re}=\text{O})}$ frequencies around 970 cm⁻¹. The $\nu_{(\text{C}=\text{O})}$ band of the benzoylthiourea (1690 cm⁻¹) shows a strong bathochromic shift as a consequence of chelate formation as has been discussed previously.⁴⁵ They appear in the spectra of the mixed-ligand complexes at approximately 1500 cm⁻¹. The mass spectra of the complexes show the expected molecular ion peaks without any ligand dissociation or formation of oligomeric complexes.

Fig. 5 depicts the molecular structure of **12b** as a model compound for this kind of complex and selected bond lengths can be found in Table 4. The Re=O distance of 1.659(5) Å is

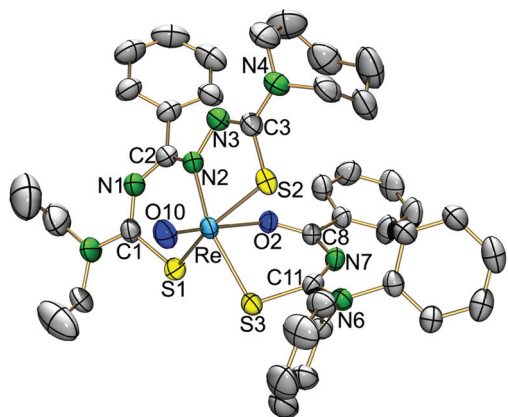


Fig. 5 Ellipsoid representations of the molecular structure of [ReO(L1b)-(Ph₂btu)] (**12b**).²¹ Hydrogen atoms have been omitted for clarity.

Table 4 Selected bond lengths (Å) and angles (°) for [ReO(L1b)(Ph₂btu)]

Re–O10	1.674(6)	S1–C1	1.733(8)
Re–S1	2.351(2)	S2–C3	1.750(9)
Re–S2	2.232(2)	S3–C11	1.760(7)
Re–N2	2.040(6)	O2–C8	1.267(8)
Re–O2	2.223(5)	N1–C2	1.31(1)
Re–S3	2.405(2)	N2–C2	1.32(1)
O10–Re–S1	101.7(1)	O10–Re–S3	98.4(2)
O10–Re–N2	102.7(2)	Re–O2–C8	130.8(5)
O10–Re–S2	98.6(2)	S1–Re–S2	159.71(8)
O10–Re–O2	175.8(2)		

within the expected range for a rhenium–oxygen double bond.²⁰ A distorted octahedral coordination geometry is found for this compound, with the oxido ligand and the oxygen atom of the bidentate Ph₂btu⁻ ligand in *trans* position to each other. The tridentate thiosemicarbazone (L1)²⁻ occupies three positions in the equatorial plane, which is completed by the sulfur atom of benzoylthiourea. The rhenium atom is situated 0.408(2) Å above this plane towards the oxido ligand. This value is less than those for the five-coordinate compounds discussed above (values between 0.68 and 0.77 Å), but more than that of the also six-coordinate compound **8b** (0.28 Å). This should have some implications on the nature of the Re–O2 bond. And indeed, the Re–O2 bond of 2.223(5) Å belongs to the longest rhenium–oxygen bonds which have been found for ligands coordinated in *trans* position to an oxido ligand in Re^V complexes. Similar values have previously only been reported for some complexes with small monodentate neutral ligands such as H₂O, MeOH or Me₂CO,²⁰ and "3 + 2" mixed-ligand complexes with tridentate thiocarbamoylbenzamidines and bidentate benzoylthioureas, the structure of which is very close to that of type **12**.⁴⁷ This means that an electron transfer from the Re=O double bond to a *trans*-Re–O single bond, which is frequently observed for alkoxido-type ligands,^{48–52} does not apply for the compounds under study.

The syntheses of a number of oxorhenium(v) mixed-ligand complexes with the *S,N,S*-tridentate thiosemicarbazones H₂L1 have demonstrated the synthetic potential of this class of ligands and recommend them for analogous studies with technetium. But in addition to this 'chemical' point of view, there is an ongoing interest in the biological behavior of these complexes, since previous studies have shown that the uncoordinated thiosemicarbazones H₂L1 as well as their rhenium complexes [ReOCl(L1)] cause a significant reduction of the growth of human MCF-7 breast cancer cells.¹⁵ The mechanism of action of some thiosemicarbazones is assumed to be due to the inhibition of ribonucleotide reductase (RR) interfering with DNA synthesis and repair, leading to apoptosis.⁵¹ The cytotoxic properties of the complex compounds under study should be influenced by chelation as well as the composition and stability of the coordination sphere of the metal.

It was found for the non-coordinated thiosemicarbazones as well as for their complexes that substitutions of the organic residues R¹ to R⁴ (see compounds **4** and **5** in Chart 1) do influence the biological activity dramatically. Some of the complexes have a lower activity, which might possibly be a hint for different uptake and distribution mechanisms for the organic compounds and their metal complexes. The replacement of the chlorido ligand (by PPh₃) and the oxido ligand by a nitrido ligand, however, terminates the cytotoxicity of the complexes completely.¹⁵ Square planar gold(III) complexes of the composition [AuX(L1)] (X = Cl, NCS) show cytotoxic effects against human MCF-7 cells in the same magnitude as the [ReOCl(L1)] compounds, while the activity increases significantly when X = CN.²² This makes it interesting to learn more about the potential biological activity of the mixed-ligand complexes of the present study.

Table 5 Cytotoxic effects (IC_{50} , μM) with estimated esd's of ligands $\text{H}_2\text{L1}$ and their complexes against MCF-7 cells

Compound	$\text{H}_2\text{L1a}$	$\text{H}_2\text{L1b}$
Ligand	0.85(± 0.07) ^a	2.43(0.28) ^a
[ReOCl(L1)] (4)	0.41(± 0.02) ^a	1.51(0.17) ^a
[ReO(SCN)(L1)] (6)	1.7(± 0.3)	2.0(0.2)
[ReO(CN)(L1)] (7)	0.6(± 0.3)	0.6(0.3)
[ReO(SCN) ₂ (HL1)] (8)	—	2.3(0.3)
[ReO(L1)(Ph ₂ btu)] (12)	22.4(± 0.3)	376(2)
Cisplatin	1.6(± 0.1)	

^a Values taken from ref. 15.

First preliminary results, the cytotoxic effects of the compounds against MCF-7 breast cancer cells as IC_{50} values, are summarized in Table 5. All thiosemicarbazones $\text{H}_2\text{L1}$ and [ReOX(L1)] (X = Cl, NCS, CN) complexes as well as [ReO-(NCS)₂(HL1b)] possess a remarkable biological activity. Changes of the alkyl/aryl substituents of the thiosemicarbazone part of the organic ligand influence the biological activity of the ligands or the complexes, but without a clear trend. Such finding is consistent with the activity of compounds 4 (see Chart 1).¹⁵

Replacement of the halide or pseudohalides by the chelating benzoylthiourea terminates the biological activity. This may suggest that the presence of a monodentate ligand (or better the possibility to abstract such a ligand *in vivo*) is an important prerequisite for the cytotoxicity of the complexes under study. This impression is supported by the fact that the cyanido compounds belong to the most active ones of the entire group. In the case of ligand $\text{H}_2\text{L1b}$ and the corresponding complex [ReO(CN)(L1b)], we can additionally consider a significant increase of the cytotoxicity for the cyanido complex. This may be explained by the combined action of two cytotoxic species inside the cells. However, further studies concerning this point and other open questions concerning the biological activity of the new class of rhenium complexes are required and are underway in our laboratories. These studies include the behavior of the complexes in aqueous media, the quest for the point of attack of the active compounds, the intracellular targets and the role of the metal ion. Experiments with structural analogue technetium complexes and/or the radioactive rhenium isotopes ¹⁸⁶Re or ¹⁸⁸Re may help to answer the open questions.

Conclusions

The five-coordinate [ReOCl(L1)] complexes show a rich ligand-exchange chemistry. Simple halide/pseudohalide exchange products can be obtained as well as nitrido complexes or mixed-chelate compounds. The coordination numbers of the product complexes are controlled by the nature of the ligands applied and the reaction route.

The cytotoxic behaviour of some of the compounds under study is remarkable. Preliminary structure-activity-studies

suggest that the observed biological activity is related to the ability of the complexes to release their anionic monodentate ligands (Cl^- , NCS^- , CN^-). Most probably, the resulting *in situ* generated cationic species are key compounds of the cytotoxic activity. Further experiments are required to understand details of the observed activity. Such an understanding, however, is a prerequisite for the optimization of the molecular framework.

Experimental section

Materials

All chemicals were reagent grade and used without further purification. The solvents were dried and used freshly distilled prior to use unless otherwise stated. $(\text{NBu}_4)[\text{ReOCl}_4]$ was prepared by a standard procedure.⁵² The thiosemicarbazones $\text{H}_2\text{L1a}$ ($\text{R}^1 = \text{Me}$, $\text{R}^2 = \text{Ph}$) and $\text{H}_2\text{L1b}$ ($\text{R}^1\text{R}^2 = -(\text{CH}_2)_6$) were prepared as reported previously.^{14,15}

Physical measurements

IR spectra were measured as KBr pellets on a Shimadzu IR Prestige-21 spectrophotometer between 400 and 4000 cm^{-1} . ¹H-NMR spectra were taken with a JEOL 400 MHz multinuclear spectrometer. ESI⁺ mass spectra were measured with an Agilent 6210 ESI-TOF (Agilent Technologies). The elemental analyses of carbon, hydrogen, nitrogen, and sulfur were determined using a Heraeus vario EL elemental analyzer. The elemental analyses of the rhenium compounds show systematically too low values for hydrogen and in some cases for carbon. This might be caused by some hydride and carbide formation. Such effects have been observed before with ligands of this type,^{14,15,22} and do not refer to impure samples. Thus, we omitted the H analyses from the experimental data given below. The values of the carbon analyses are uncorrected and some results of high resolution mass spectra are supplied in order to verify the identity of the complexes unambiguously.

Syntheses

[ReO(NCS)(L1)] type complexes. NH_4SCN (0.075 mmol) dissolved in 1 mL MeOH was added to a solution containing 0.05 mmol of [ReOCl(L1)] in 1 mL CH_2Cl_2 . The resulting solution was stirred for 2 h at room temperature. After this time, the solvent was completely removed in a vacuum and the remaining solid was repeatedly washed with MeOH, filtered off and dried in a vacuum. Single-crystals suitable for X-ray diffraction were obtained by recrystallization from CH_2Cl_2 -MeOH.

[ReO(NCS)(L1a)] (6a). Color: red. Yield: 82% (27 mg). Anal. Calcd for $\text{C}_{21}\text{H}_{23}\text{N}_6\text{OReS}_3$ (657.84): C, 38.3; N, 12.8; S, 14.6. Found: C, 38.4; N, 12.7; S, 15.2%. IR ($\nu_{\text{max}}/\text{cm}^{-1}$): 2068 vs ($\text{C}\equiv\text{N}$, isothiocyanato), 1559 m ($\text{C}=\text{N}$, ligand), 976 s ($\text{Re}=\text{O}$). ¹H NMR (CDCl_3 , ppm): 1.29–1.37 (m, 6H, CH_3), 3.32 (s, 3H, NCH_3), 3.88–4.03 (m, 4H, CH_2), 7.16–7.22 (m, 3H, Ph), 7.1 (t, $J = 7.6$ Hz, 2H, Ph), 7.36–7.45 (m, 3H, Ph), 7.69 (d, $J = 6.8$ Hz, 2H, Ph). ESI⁺ MS (m/z , assignment): 600 [$\text{M} - \text{Cl}$]⁺, 682 [$\text{M} + \text{Na}$]⁺, 698 [$\text{M} + \text{K}$]⁺, 1258 [$2\text{M} - \text{SCN}$]⁺.

[ReO(NCS)(L1b)] (6b). Color: red. Yield: 95% (31 mg). Anal. Calcd for $C_{22}H_{31}N_7OReS_4$ (649.86): C, 37.0; N, 12.9; S, 14.8. Found: C, 36.9; N, 12.8; S, 14.5%. IR ($\nu_{\max}/\text{cm}^{-1}$): 2064 vs (C≡N, isothiocyanato), 1558 vs (C=N, ligand), 980 s (Re=O). ^1H NMR (CDCl_3 , ppm): 1.27–1.36 (m, 6H, CH_3), 1.46–1.59 (m, 8H, CH_2 azepine), 3.51–3.61 (m, 4H, N- CH_2 azepine), 3.87–3.94 (m, 4H, CH_2), 7.19–7.38 (m, 3H, Ph), 7.60 (d, $J = 8.0$ Hz, 2H, Ph). ESI+ MS (m/z , assignment): 624 $[\text{M} - \text{Cl} + \text{MeOH}]^+$ + 652 $[\text{M} + \text{H}]^+$, 674 $[\text{M} + \text{Na}]^+$, 690 $[\text{M} + \text{K}]^+$.

[ReO(CN)(L1)] type complexes. KCN (0.075 mmol) dissolved in 2 mL MeOH was added to a solution containing the desired $[\text{ReOCl}(\text{L1})]$ complex (0.05 mmol) in 1 mL CH_2Cl_2 . The resulting mixture was stirred for 2 h at room temperature. After removal of the solvents in a vacuum, the resulting solid was dispersed in 2 mL water and extracted with CH_2Cl_2 (2×2 mL). The organic phase was separated, dried with MgSO_4 and the solvent was removed under reduced pressure. This results in pure red solids. Single-crystals of $[\text{ReO}(\text{L1a})(\text{CN})]$ suitable for X-ray diffraction were obtained by recrystallization from CH_2Cl_2 -*n*-hexane.

[ReO(CN)(L1a)] (7a). Color: red. Yield: 93% (29 mg). Anal. Calcd for $C_{21}H_{23}N_6OReS_2$: C, 40.3; N, 13.4; S, 10.3%. Found: C, 40.2; N, 13.2; S, 10.4%. IR ($\nu_{\max}/\text{cm}^{-1}$): 2128 w (C≡N, cyanido), 1559 vs (C=N), 989 vs (Re=O). ^1H NMR (CDCl_3 , ppm): 1.35 (m, 6H, CH_3), 3.36 (s, 3H, NCH_3), 3.81–3.91 (m, 2H, CH_2), 3.95–4.19 (m, 2H, CH_2), 7.16–7.23 (m, 3H, Ph), 7.30 (t, $J = 7.8$ Hz, 2H, Ph), 7.37–7.50 (m, 3H, Ph), 7.78 (d, $J = 7.0$ Hz, 2H, Ph). ESI+ MS (m/z , assignment): 627 $[\text{M} + \text{H}]^+$, 649 $[\text{M} + \text{Na}]^+$, 665 $[\text{M} + \text{K}]^+$, 1275 $[2\text{M} + \text{Na}]^+$.

[ReO(CN)(L1b)] (7b). Color: red. Yield: 81% (25 mg). Anal. Calcd for $C_{20}H_{27}N_6OReS_2$ (617.80): C, 38.9; N, 13.6; S, 10.4. Found: C, 39.0; N, 13.4; S, 10.6%. IR ($\nu_{\max}/\text{cm}^{-1}$): 2122 w (C≡N, cyanido), 1570 vs (C=N), 990 vs (Re=O). ^1H NMR (CDCl_3 , ppm): 1.30–1.35 (m, 6H, CH_3), 1.36–1.62 (m, 8H, CH_2 azepine), 3.57–3.62 (m, 4H, N- CH_2 azepine), 3.82–4.12 (m, 4H, CH_2), 7.32–7.42 (m, 3H, Ph), 7.70 (d, $J = 7.0$ Hz, 2H, Ph). ESI+ MS (m/z , assignment): 619 $[\text{M} + \text{H}]^+$, 641 $[\text{M} + \text{Na}]^+$, 657 $[\text{M} + \text{K}]^+$.

[ReO(NCS)₂(HL1b)] (8b). $\text{H}_2\text{L1b}$ (0.1 mmol) was added to a solution of $(\text{NBu}_4)[\text{ReOCl}_4]$ (0.1 mmol) in 1 mL and stirred for 2 h at room temperature. Then, NH_4SCN (0.4 mmol) in 1 mL MeOH was added and the resulting mixture was stirred for one more hour. This results in the precipitation of a brown solid compound, which was filtered off, washed with MeOH, *n*-hexane and dried under vacuum. Single-crystals suitable for an X-ray study were obtained by recrystallization from CH_2Cl_2 -MeOH. Color: brown. Yield: 97% (69 mg). Anal. Calcd for $C_{21}H_{28}N_7ReS_4$ (692.95): C, 36.5; N, 13.5; S, 17.7. Found: C, 35.7; N, 13.6; S, 18.1%. IR ($\nu_{\max}/\text{cm}^{-1}$): 3089 w (N-H), 2102 vs (C≡N, isothiocyanate), 2081 vs (C≡N, isothiocyanato), 1590 vs (C=N, ligand), 965 s (Re=O). ^1H NMR (CDCl_3 , ppm): 1.27–1.35 (m, 6H, CH_3), 1.47–1.60 (m, 8H, CH_2 azepine), 3.54–3.58 (m, 4H, N- CH_2 azepine), 3.90–3.93 (m, 4H, CH_2), 7.32–7.37 (m, 3H, Ph), 7.60 (d, $J = 7.7$ Hz, 2H, Ph). ESI+ MS (m/z , assignment): 651 $[\text{M} - \text{NCS}]^+$, 1242 $[2\text{M} - 3(\text{NCS}) - 2\text{H}]^+$, 1301 $[2\text{M} - 2\text{NCS} - \text{H}]^+$.

[ReO(NCS)(L1b)(dmsO-kO)] (9b). A sample of $[\text{ReO}(\text{NCS})_2(\text{HL1b})]$ was recrystallized from a DMSO–MeOH (1 : 2) mixture. Color: purple. Yield: 90% (65 mg). Anal. Calcd for $C_{22}H_{33}N_6O_2ReS_4$ (727.99): C, 36.3; N, 11.5; S, 17.6. Found: C, 36.0; N, 11.9; S, 18.0. IR ($\nu_{\max}/\text{cm}^{-1}$): 2074 vs (C≡N, isothiocyanato), 1524 vs (C=N, ligand), 990 (S=O), 971 s (Re=O). ^1H NMR (CDCl_3 , ppm): 1.29 (t, $J = 7.2$ Hz, 3H, CH_3), 1.34 (t, $J = 7.0$ Hz, 3H, CH_3), 1.43–1.63 (m, 8H, CH_2 azepine), 2.55 (6H, CH_3 dmsO), 3.50–3.63 (m, 4H, NCH_2 azepine), 3.88–3.98 (m, 4H, CH_2), 7.40–7.55 (m, 3H, Ph), 7.55 (d, $J = 6.1$ Hz, 2H, Ph). ESI+ MS (m/z , assignment): 1242 $[2\text{M} - 2(\text{dmsO}) - (\text{NCS})]^+$.

[ReO(N₃)(L1b)] (10b). Method A. $\text{H}_2\text{L1b}$ (0.05 mmol) was added to a solution of $(\text{NBu}_4)[\text{ReOCl}_4]$ (0.05 mmol) in 1 mL MeOH and the mixture was stirred for 1 h at room temperature. Then, a solution of NaN_3 (0.15 mmol) in 1 mL MeOH was added and the stirring was continued for one more hour. A dark brown precipitate was formed during this time, which was filtered off, washed with H_2O (3×1 mL) and MeOH and dried in a vacuum. Yield: 75% (24 mg).

Method B. A solution of NaN_3 (0.1 mmol) in 2 mL MeOH was added to a solution of $[\text{ReOCl}(\text{L1b})]$ (0.05 mmol) in 0.5 mL CH_2Cl_2 . The resulting mixture was stirred for a period of 1 h, during which a brown solid precipitated. This precipitate was filtered off and treated as described for method A. Yield: 85% (27 mg).

Color: dark brown. IR ($\nu_{\max}/\text{cm}^{-1}$): 2059 vs (N≡N), 1555 s (C=N), 1512 vs, 1454 s (C=C), 973 m (Re=O). ^1H NMR (CDCl_3 , ppm): 1.21–1.46 (m, 6H, CH_3), 1.47–1.70 (m, 8H, CH_2 azepine), 3.46–3.63 (m, 4H, N- CH_2 azepine), 3.65–4.13 (m, 4H, CH_2), 7.30–7.43 (m, 3H, Ph), 7.61–7.71 (m, 2H, Ph). UV-Vis (CH_2Cl_2) [λ_{\max}/nm (ϵ): 379 (17 274).

[{ReN(HL1b)}₂O] (11b). $[\text{ReO}(\text{N}_3)(\text{L1b})]$ was dissolved in warm CH_2Cl_2 -MeCN or CH_2Cl_2 -MeOH mixtures and slowly cooled for crystallization. A change of color from brown to red was observed and finally a crystalline material was obtained in almost quantitative yield. Color: red. Anal. Calcd for $C_{38}H_{56}N_{12}ORe_2S_4$ (1197.60): C, 38.1; N, 14.0; S, 10.7%. Found: C, 37.0; N, 15.1; S, 11.0%. IR ($\nu_{\max}/\text{cm}^{-1}$): 1558 (C=N), 1516, 1488 (C=C), 1028 (Re≡N), 694 (Re–O–Re). ^1H NMR (CDCl_3 , ppm): 1.36 (t, $J = 8$ Hz, 6H, CH_3), 1.41 (t, $J = 8$ Hz, 6H, CH_3), 1.51–1.71 (m, 16H, CH_2 azepine + H_2O), 3.62–3.71 (m, 8H, N- CH_2 azepine), 3.93–4.11 (m, 8H, CH_2), 7.37–7.44 (m, 3H, Ph), 7.67 (d, $J = 8$ Hz, 2H, Ph). ESI+ MS (m/z , assignment): 1198 $[\text{M} + \text{H}]^+$. UV-Vis (CH_2Cl_2) [λ_{\max}/nm (ϵ): 258 (56 886), 395 (22 635).

Synthesis of the mixed-chelate complexes. $\text{H}_2\text{L1}$ (0.1 mmol) was added to a solution of $(\text{NBu}_4)[\text{ReOCl}_4]$ in 2 mL MeOH and stirred for 2 h at room temperature. The formed precipitate was re-dissolved by the addition of 2 mL CH_2Cl_2 . Then, HPh_2btu (0.1 mmol, 33.2 mg) and 3 drops of Et_3N were added. The solution was stirred for one more hour and then the solvent was removed in a vacuum. The remaining solid was washed with 1 mL MeOH, filtered and recrystallized from a minimum amount of a MeOH– CH_2Cl_2 (1 : 2) mixture. During cooling in a refrigerator, crystalline precipitates were formed, which were filtered off and dried in a vacuum.

Table 6 X-ray structure data collection and refinement parameters

	6a	6b	7a	8b	9b	11b	12b
Formula	C ₂₁ H ₂₃ N ₆ OReS ₃	C ₂₀ H ₂₇ N ₆ OReS ₃	C ₂₁ H ₂₃ N ₆ OReS ₂	C ₂₁ H ₂₈ N ₇ OReS ₄	C ₂₂ H ₃₃ N ₆ O ₂ ReS ₄	C ₄₀ H ₆₀ Cl ₄ N ₁₂ ORe ₂ S ₄	C ₃₉ H ₄₂ N ₇ O ₂ ReS ₃
Fw	657.83	649.86	625.77	708.94	727.99	1367.44	923.18
System	Triclinic	Monoclinic	Monoclinic	Monoclinic	Triclinic	Triclinic	Triclinic
Space group	P1	P2 ₁ ^a	P2 ₁ /c	P2 ₁ /n	P1	P1	P1
a (Å)	11.208(1)	9.336(5)	9.9759(6)	14.2273(15)	8.5513(6)	8.2495(10)	8.2241(7)
b (Å)	14.146(1)	11.117(5)	10.7569(7)	12.9103(9)	14.4707(11)	12.7783(15)	11.7497(8)
c (Å)	16.761(1)	11.842(5)	21.8824(14)	14.6062(18)	24.0433(17)	13.0830(15)	20.5128(17)
α (°)	101.91(1)				76.669(6)	81.510(9)	93.909(6)
β (°)	90.36(1)	102.937(5)	91.5310(10)	93.9810(10)	83.918(6)	74.673(10)	99.602(7)
γ (°)	111.66(1)				89.555(6)	78.558(10)	93.003(6)
V (Å ³)	2406.8(3)	1197.9(10)	2347.4(3)	2676.4(5)	2878.3(4)	1297.0(3)	1945.7(3)
Z	4	2	4	4	4	1	2
ρ _{calcd} (g cm ⁻³)	1.815	1.802	1.771	1.759	1.680	1.751	1.576
M (mm ⁻¹)	5.335	5.358	5.380	4.881	4.542	5.074	3.328
θ Range	1.79 to 29.24	1.76 to 29.22	1.86 to 29.28	1.93 to 29.22	1.75 to 29.30	1.62 to 29.26	1.94 to 29.30
Indices	-15 ≤ h ≤ 12, -19 ≤ k ≤ 19, -23 ≤ l ≤ 22	-12 ≤ h ≤ 10, -15 ≤ k ≤ 13, -16 ≤ l ≤ 16	-13 ≤ h ≤ 8, -14 ≤ k ≤ 13, -29 ≤ l ≤ 29	-19 ≤ h ≤ 19, -17 ≤ k ≤ 15, -16 ≤ l ≤ 20	-11 ≤ h ≤ 9, -19 ≤ k ≤ 19, -32 ≤ l ≤ 33	-9 ≤ h ≤ 11, -17 ≤ k ≤ 17, -17 ≤ l ≤ 17	-11 ≤ h ≤ 10, -14 ≤ k ≤ 16, -28 ≤ l ≤ 28
Reflections collected	25 604	8209	14 594	17 994	31 690	13 431	20 481
Unique/R _{int}	12 813/0.0928	5437/0.0909	6276/0.1038	7171/0.1507	15 314/0.0971	6875/0.0627	10 390/0.0922
Data	12 813	5437	6276	7171	15 314	6875	10 390
Restraints	0	1	0	0	0	0	0
Parameters	584	283	284	309	639	293	472
Abs. corr.	Integration	Integration	Integration	Integration	Integration	Integration	None
T _{max} /T _{min}	0.5461/0.3029	0.7524/0.5070	0.5387/0.1709	0.8647/0.6603	0.5883/0.4135	0.7013/0.3046	—
R ₁ [I > 2σ(I)]	0.0431	0.0582	0.0601	0.0525	0.0497	0.0407	0.0569
wR ₂ [I > 2σ(I)]	0.0872	0.1356	0.1524	0.1128	0.0952	0.0973	0.1196
GOF on F ²	0.824	0.997	1.056	0.791	0.867	1.018	0.979
CCDC code	911727	911728	911729	911730	911731	911732	911733

^a Flack parameter: -0.01(2).

[**ReO(L1a)(Ph₂btu)**] (**12a**). Color: deep purple. Yield: 85% (80 mg). Anal. Calcd for C₄₁H₄₁N₇O₂ReS₃ (946.20): C, 52.0; N, 10.4; S, 10.2. Found: C, 49.4; N, 9.9; S, 10.3%. ¹H NMR (CDCl₃, ppm): 1.14–1.26 (m, 6H, CH₃), 3.31 (s, 3H, N–CH₃), 3.61–3.71 (m, 2H, N–CH₂), 3.89–4.01 (m, 2H, N–CH₂), 7.03 (t, *J* = 7.8 Hz, Ph), 7.13–7.45 (m, 21H, Ph), 7.72 (dd, *3J* = 6.6 Hz, *4J* = 2.0 Hz, 2 H, Ph). ESI+ MS (*m/z*): 932 [M + H]⁺, 954 [M + Na]⁺, 970 [M + K]⁺.

[**ReO(L1b)(Ph₂btu)**] (**12b**). Color: deep purple. Yield: 89% (83 mg). Anal. Calcd for C₄₀H₄₅N₇O₂ReS₃ (938.24): C, 51.2; N, 10.5; S, 10.3. Found: C, 50.2; N, 10.4; S, 10.5. ¹H NMR (CDCl₃, ppm): 1.16–1.23 (m, 6H, CH₃), 1.41 (s, br, 3H, CH₂, azepine), 1.49–1.53 (m, 5H, CH₂, azepine), 3.52–3.71 (m, 6H, N–CH₂, azepine + NCH₂CH₃), 3.90–3.98 (m, 2H, N–CH₂), 7.01 (t, *J* = 7.8 Hz, Ph), 7.18–7.55 (m, 16H, Ph), 7.67 (dd, *J* = 7.6 Hz, *4J* = 2.0 Hz, 2H, Ph). ESI+ MS (*m/z*): 924 [M + H]⁺.

X-ray crystallography

The intensities for the X-ray determinations were collected on a STOE IPDS 2T instrument with Mo K α radiation (λ = 0.71073 Å). Standard procedures were applied for data reduction and absorption correction. Structure solution and refinement were performed with SHELXS-97 and SHELXL-97.⁵³ Hydrogen atom positions were calculated for idealized positions and treated with the “riding model” option of SHELXL. More details on data collections and structure calculations are contained in Table 6.

Biochemicals and biological studies

Cell culture conditions. The human MCF-7 breast cancer cell line was obtained from the American type Culture Collection (ATCC). This cell line was maintained as a monolayer culture in L-glutamine containing Dulbecco's Modified Eagle's Medium (DMEM) with 4.5 g L⁻¹ glucose (PAA Laboratories GmbH, Austria), supplemented with 10% fetal calf serum (FCS; Gibco, Germany) using 25 cm² culture flasks in a humidified atmosphere (5% CO₂) at 37 °C. The cell lines were passaged twice a week after previous treatment with trypsin (0.05%)/ethylenediamine tetraacetic acid (0.02% EDTA; Boehringer, Germany). Jurkat cells were purchased from German Collection of Microorganisms and Cell Culture (Deutsche Sammlung von Mikroorganismen und Zellkulturen, Braunschweig), DSMZ No ACC 282, LOT 7. The cells were maintained in a RPMI 1640 (PAA) medium supplemented with 10% fetal calf serum (PAA), 37 °C, 5% CO₂ and maximum humidity.

In vitro chemosensitivity assay. The *in vitro* testing of the substances for antitumor activity in adherent growing cell lines was carried out on exponentially dividing human cancer cells according to a previously published microtiter assay.^{54,55} Exponential cell growth was ensured during the whole time of incubation. Briefly, 100 μ L of a cell suspension was placed in each well of a 96-well microtiter plate at 7200 cells per mL of culture medium and incubated at 37 °C in a humidified atmosphere (5% CO₂) for 3 d. By removing the old medium

and adding 200 μ L of fresh medium containing an adequate volume of a stock solution of the metal complex, the desired test concentration was obtained. Cisplatin was dissolved in dimethylformamide (DMF) while dimethylsulfoxide (DMSO) was used for all other compounds. Eight wells were used for each test concentration and for the control, which contained the corresponding amount of DMF and DMSO, respectively. The medium was removed after reaching the appropriate incubation time. Subsequently, the cells were fixed with a solution of 1% (v/v) glutaric dialdehyde in phosphate buffered saline (PBS) and stored under PBS at 4 °C. Cell biomass was determined by means of a crystal violet staining technique as described earlier.⁵⁶ The effectiveness of the complexes is expressed as corrected *T/C*_{corr} [%] or τ [%] values according to the following equation:

$$\text{cytostatic effect : } T/C_{\text{corr}}[\%] = [(T - C_0)/(C - C_0)] \times 100$$

$$\text{cytotoxic effect : } \tau[\%] = [(T - C_0)/C_0] \times 100$$

whereby *T*_(test) and *C*_(control) are the optical densities at 590 nm of crystal violet extract of the cells in the wells (*i.e.* the chromatin-bound crystal violet extracted with ethanol (70%) with *C*₀ being the density of the cell extract immediately before treatment. For the automatic estimation of the optical density of the crystal violet extract in the wells, a microplate autoreader (Flashscan S 12; Analytik Jena, Germany) was used.

Acknowledgements

We gratefully acknowledge financial support of DAAD, NAFOSTED (HHN, project 104.02-2010.31), CAPES (PROBRAL) and FAPESP (Process 2011/16380-1).

Notes and references

- 1 J. S. Casas, M. S. García-Tasende and J. Sordo, *Coord. Chem. Rev.*, 2000, **209**, 197.
- 2 Y. Yu, D. S. Kalinowski, Z. Kovacevic, A. R. Siafakas, P. J. Jansson, C. Stefani, D. P. Lovejoy, P. C. Sharpe, P. V. Bernhardt and D. R. Richardson, *J. Med. Chem.*, 2009, **52**, 5271.
- 3 D. L. Klayman, J. P. Scovill, J. F. Bartosevich and C. J. Mason, *J. Med. Chem.*, 1979, **22**, 1367.
- 4 H. Beraldo and D. Gambino, *Mini-Rev. Med. Chem.*, 2004, **4**, 31.
- 5 M. Christlieb and J. Dilworth, *Chem.-Eur. J.*, 2006, **12**, 6194.
- 6 F. R. Pavan, P. I. S. Maia, S. R. A. Leite, V. M. Deflon, A. A. Batista, D. N. Sato, S. G. Franzblau and C. Q. F. Leite, *Eur. J. Med. Chem.*, 2010, **45**, 1898.
- 7 P. J. Blower and S. Prakash, in *Perspectives on Bioinorganic Chemistry*, ed. R. W. Hay, H. R. Dilworth and K. B. Nolan, JAI Press Inc., 1999, vol. 4, pp. 91–143.
- 8 E. Deutsch, K. Libson, J.-L. Vanderheyden, A. Ketring and H. R. Maxon, *Nucl. Med. Biol.*, 1986, **13**, 465.

- 9 S. Jurisson, D. Berning, W. Jia and D. Ma, *Chem. Rev.*, 1993, **93**, 1137.
- 10 U. Abram and R. Alberto, *J. Braz. Chem. Soc.*, 2006, **17**, 1486.
- 11 P. S. Donnelly, *Dalton Trans.*, 2010, **39**, 999.
- 12 S. Bhattacharyya and M. Dixit, *Dalton Trans.*, 2011, **40**, 6112.
- 13 R. Alberto and U. Abram, in *Handbook of Nuclear Chemistry*, ed. A. Vértes, S. Nagy, Z. Klencsár, R. G. Lovas and F. Rösch, Springer, US, 2011, vol. 4, pp. 2073–2120.
- 14 H. H. Nguyen, P. I. S. Maia, V. M. Deflon and U. Abram, *Inorg. Chem.*, 2009, **48**, 25.
- 15 H. H. Nguyen, J. J. Jegathesh, P. I. S. Maia, V. M. Deflon, R. Gust, S. Bergemann and U. Abram, *Inorg. Chem.*, 2009, **48**, 9356.
- 16 A. R. Cowley, J. R. Dilworth, P. S. Donnelly and J. Woollard-Shore, *J. Chem. Soc., Dalton Trans.*, 2003, 748.
- 17 I. Garcia Santos and U. Abram, *Z. Anorg. Allg. Chem.*, 2004, **630**, 697.
- 18 B. M. Paterson, J. M. White and P. S. Donnelly, *Dalton Trans.*, 2010, **39**, 2831.
- 19 K. Nakamoto, *Infrared and Raman Spectra of Inorganic and Coordination Compounds, Part B*, John Wiley & Sons, New Jersey, 2009.
- 20 U. Abram, Rhenium. in *Comprehensive Coordination Chemistry II*, Elsevier, 2003, vol. 5, pp. 271–402.
- 21 L. J. Farrugia, *J. Appl. Crystallogr.*, 1999, **32**, 837.
- 22 P. I. d. S. Maia, H. H. Nguyen, D. Ponader, A. Hagenbach, S. Bergemann, R. Gust, V. M. Deflon and U. Abram, *Inorg. Chem.*, 2012, **51**, 1604.
- 23 A. Davison, A. G. Jones, L. Müller, R. Tatz and H. S. Trop, *Inorg. Chem.*, 1981, **20**, 1160.
- 24 K. Brandenburg, *DIAMOND, vers. 3.2i*, Crystal Impact GbR, Bonn, Germany.
- 25 M. B. Hursthouse and K. M. A. Malik, *J. Chem. Soc., Dalton Trans.*, 1979, 409.
- 26 P. A. Kozmin, M. D. Surazhskaya and T. B. Larina, *Koord. Khim.*, 1979, **5**, 598.
- 27 J. Jacob, G. Lente, I. A. Guzei and J. H. Espenson, *Inorg. Chem.*, 1999, **38**, 3762.
- 28 Z. Zheng, T. G. Gray and R. H. Holm, *Inorg. Chem.*, 1999, **38**, 4888.
- 29 M. Casanova, E. Zangrando, F. Munini, E. Iengo and E. Alessio, *Dalton Trans.*, 2006, 5033.
- 30 Z. Zheng and R. H. Holm, *Inorg. Chem.*, 1997, **36**, 5173.
- 31 N. Q. Mendez, A. M. Arif and J. A. Gladysz, *Organometallics*, 1991, **10**, 2199.
- 32 S. Ritter and U. Abram, *Inorg. Chim. Acta*, 1994, **215**, 159.
- 33 H. H. Nguyen, J. Grewe, J. Schroer, B. Kuhn and U. Abram, *Inorg. Chem.*, 2008, **47**, 5136.
- 34 J. Schroer, S. Wagner and U. Abram, *Inorg. Chem.*, 2010, **49**, 10694.
- 35 K. Dehnicke and J. Strähle, *Angew. Chem.*, 1981, **93**, 451.
- 36 K. Dehnicke and J. Strähle, *Angew. Chem.*, 1992, **104**, 978.
- 37 U. Abram, B. Schmidt-Brücken, A. Hagenbach, M. Hecht, R. Kirmse and A. Voigt, *Z. Anorg. Allg. Chem.*, 2003, **629**, 838.
- 38 U. Abram, M. Braun, S. Abram, R. Kirmse and A. Voigt, *J. Chem. Soc., Dalton Trans.*, 1998, 231.
- 39 H. Braband, E. Oehlke and U. Abram, *Z. Anorg. Allg. Chem.*, 2006, **632**, 1051.
- 40 H. Braband, E. Yegen, E. Oehlke and U. Abram, *Z. Anorg. Allg. Chem.*, 2005, **631**, 2408.
- 41 J. Baldas, S. F. Colmanet and M. F. Mackay, *J. Chem. Soc., Dalton Trans.*, 1988, 1725.
- 42 T. Nicholson, D. J. Kramer, A. Davison and A. G. Jones, *Inorg. Chim. Acta*, 2001, **316**, 110.
- 43 J. Baldas, J. F. Boas, S. F. Colmanet and G. A. Williams, *J. Chem. Soc., Dalton Trans.*, 1992, 2845.
- 44 J. Baldas, J. F. Boas, J. Bonnyman, S. F. Colmanet and G. A. Williams, *Chem. Commun.*, 1990, 1163.
- 45 H. H. Nguyen and U. Abram, *Inorg. Chem.*, 2007, **46**, 5310.
- 46 H. H. Nguyen and U. Abram, *Z. Anorg. Allg. Chem.*, 2008, **634**, 1560.
- 47 H. H. Nguyen, V. M. Deflon and U. Abram, *Eur. J. Inorg. Chem.*, 2009, 3179.
- 48 S. Abram, U. Abram, E. Schulz Lang and J. Strähle, *Acta Crystallogr., Sect. C: Cryst. Struct. Commun.*, 1995, **51**, 1078 and references cited therein.
- 49 A. Paulo, A. Domingos, J. Marcalo, A. Pires de Matos and I. Santos, *Inorg. Chem.*, 1995, **34**, 2113.
- 50 H. Braband, O. Blatt and U. Abram, *Z. Anorg. Allg. Chem.*, 2006, **632**, 2251.
- 51 J. Chen, Y.-W. Huang, G. Liu, Z. Afrasiabi, E. Sinn, S. Padhye and Y. Ma, *Toxicol. Appl. Pharmacol.*, 2004, **197**, 40.
- 52 R. Alberto, R. Schibli, A. Egli, P. A. Schubiger, W. A. Hermann, G. Artus, U. Abram and T. A. Kaden, *J. Organomet. Chem.*, 1995, **493**, 119.
- 53 G. M. Sheldrick, *SHELXS-97 and SHELXL-97, Programs for the solution and refinement of crystal structures*, University of Göttingen, Göttingen, Germany, 1997.
- 54 G. Bernhart, H. Reile, H. Birnböck, T. Spruss and H. Schönenberger, *J. Cancer Res. Clin. Oncol.*, 1992, **118**, 35.
- 55 H. Reile, H. Birnböck, G. Bernhart, T. Spruss and H. Schönenberger, *Anal. Biochem.*, 1990, **187**, 262.
- 56 J. A. Marmur, *J. Mol. Biol.*, 1961, **3**, 208.